Neuroradiology (1985) 27: 208-213

Neuroradiology

MRI (NMR) in the diagnosis of brain-stem tumors

G. B. Bradac[1], W. Schörner[2], A. Bender[1], and R. Felix[2]

[1]Section of Neuroradiology, Department of Radiology, Steglitz Clinic, and
[2]Department of Radiology, Charlottenburg Clinic Free University Berlin

Summary. Patients with a brain-stem tumor were studied with NMR. The full extent of the lesion as well as its relationship with the adjacent structures was clearly demonstrated in all cases. Although NMR is, in many aspects, superior to CT and angiography, these examinations remain useful complementary methods.

Key words: MRI - NMR - brain stem - brain tumor

Since the introduction of NMR (now often known as Magnetic Resonance Imaging (MRI) into clinical practice, there have already been reports [1, 2, 4] about its diagnostic value. It is, however, not yet definitely established which kind of pathology and which part of the nervous system will derive the greatest benefit from this technique. In December 1983, an NMR scanner was installed in the Radiological Department of Charlottenburg Clinic of the Free University of Berlin.

Since then, about 700 patients with different neurologic diseases have been examined. Nine patients with a tumor affecting the brain stem have been selected for this study.

Table 1. Patients with brain-stem tumor studied with NMR

Patient	Age (year) sex	Localization	Histology
1	10 M	Pineal region-Midbrain-Pons	Pineocytoma
2	9 F	Pineal region-Midbrain	Ependymoblastoma
3	32 M	Thalamic area-Midbrain	Astrocytoma I-II
4	12 M	Midbrain-Pons-Medulla oblongata	Glioblastoma
5	40 M	Midbrain-Pons-Medulla oblongata	Astrocytoma I-II
6	13 F	Pons-Medulla oblongata-Spinal cord	Gangliocytoma
7	31 M	Pons-Medulla oblongata	Astrocytoma I-II
8	52 M	Medulla oblongata-Left cerebellar hemisphere	Astrocytoma III
9	20 M	Medulla oblongata-Vermis inferior	Angioblastoma

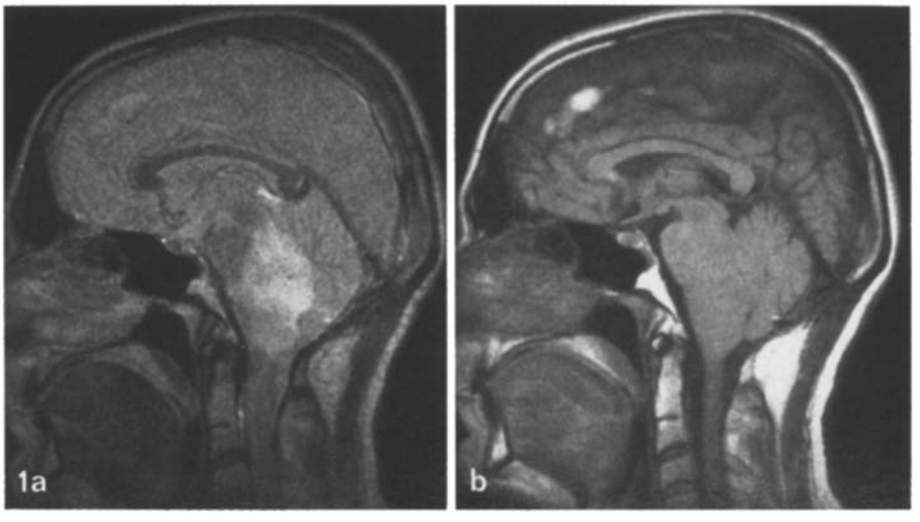

Fig. 1 a and b. case 5. Brainstem astrocytoma **a** SE 1600/70. The tumor *(white area)* displays an increase of signal intensity in T2 weighted spin-echo. It infiltrates the midbrain, the pons, and the medulla oblongata. **b** SE 400/35. The tumor is now not directly visible, but there is an evident enlargement of the pons and medulla oblongata. The IV. ventricle is no longer recognizable. The cerebellum is shifted dorsally. A small haemorrhage is visible in the cerebral hemisphere due to ventricle puncture

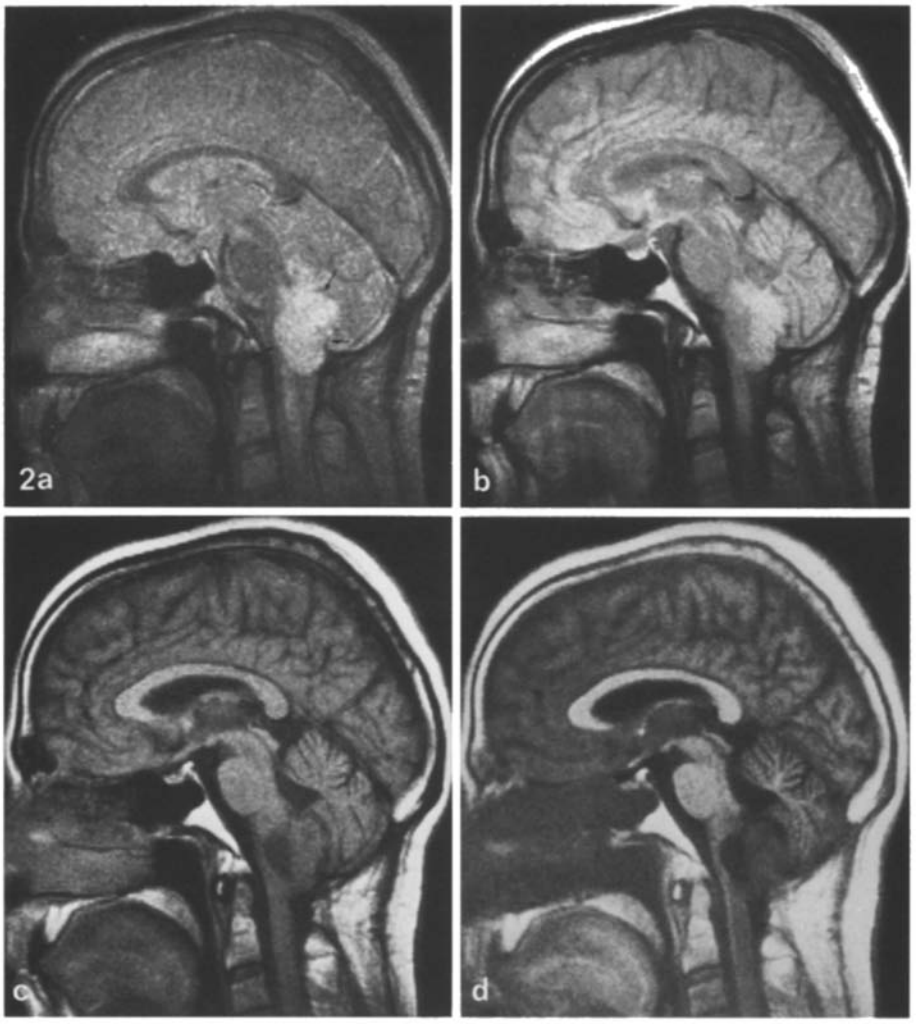

Fig. 2 a–d. case 9. Angioblastoma involving medulla oblongata and vermis inferior. **a** SE 1600/70. The tumor is clearly visible (→). It shows a lengthening of T2 *(white area)* **b** SE 1600/35. The tumor is now less well visible. But two different parts of the lesion are recognizable. The anatomical details are shown better. **c** SE 400/35. On this T1 weighted sequence the rostral part of the tumor (cystic) has a longer T1 than the dorsal part (solid). The anatomical structures are clearly visible. A compression of the IV. ventricle is clearly recognizable. **d** IR 1500/400. Excellent demonstration of anatomical details. The tumor shows lengthening of T1 which is more evident in the cystic portion. A questionable decreased signal intensity inside the spinal cord is visible which could be a sign of widening of the canalis centralis

Material and method

NMR images were obtained with a superconducting whole body scanner (Magnetom, Siemens) operating at 0.35 Tesla. The NMR coil (diameter: 25 cm) used for brain imaging had a nominal spatial resolution of 1 mm in the section imaged (slice thickness: 10 mm). Axial and sagittal sections were obtained through the brain using a multiple slice technique. Spin-echo (SE) pulse sequences with different repetition times (TR) and echo delay times (TE) were applied. For simplicity of reference, sequences will be referred to in the following format: SE TR/TE. Each examination involved the use of T1-weighted (SE 400/35), proton-density-weighted (SE 1600/35), and T2-weighted scans (SE 1600/70). Scanning time was 4 to 14 min, depending on the pulse sequences applied. In addition, we used inversion recovery (IR) sequence (1500/400/35) in one patient. All patients underwent CT and angiography, whose findings were compared with those of NMR. The diagnosis of tumor was confirmed by surgery. Table 1 shows the localization of the lesion and the histology in all patients.

Results

1. The tumor could be precisely diagnosed in all cases.

2. Different spin-echo sequences were necessary to recognize the tumor itself, the various components of it, the deformation of the brain stem and the compression of the adjacent structures (Figs. 1, 2).

3. The tumor showed a lengthening of T2 and T1 in all cases. In one child, the increase of signal intensity of T2-weighted SE was only partially appreciable due to movement artefacts. In general, the tumor itself was better recognizable with the T2-weighted SE 1600/70, while, with the SE 1600/35, the anatomical structures were better visible. With the T1-weighted SE 400/35, the tumor was generally

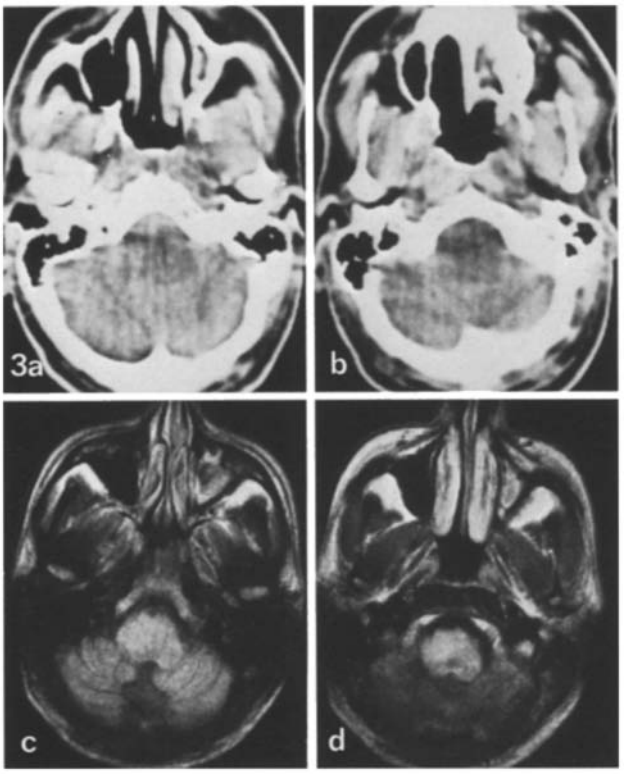

Fig. 3a–f. case 7. Astrocytoma involving pons and medulla oblongata. **a, b** On CT, only an area of decreased density in the region corresponding to the medulla oblongata was discernible. **c, d** The same axial planes on NMR (SE 1600/35). Evident enlargement of medulla oblongata. **e, f** Sagittal planes; **e** SE 1600/35. Enlargement of the medulla oblongata (↔). Vallecula and IV. ventricle slightly shifted dorsally. **f** SE 1600/70. With this sequence, the anatomical structures are less well recognizable. The tumor extending partially into the pons displays a long T2 *(white area)*. Note, in the supratentorial area the internal cerebral vein appearing white due to a long T2

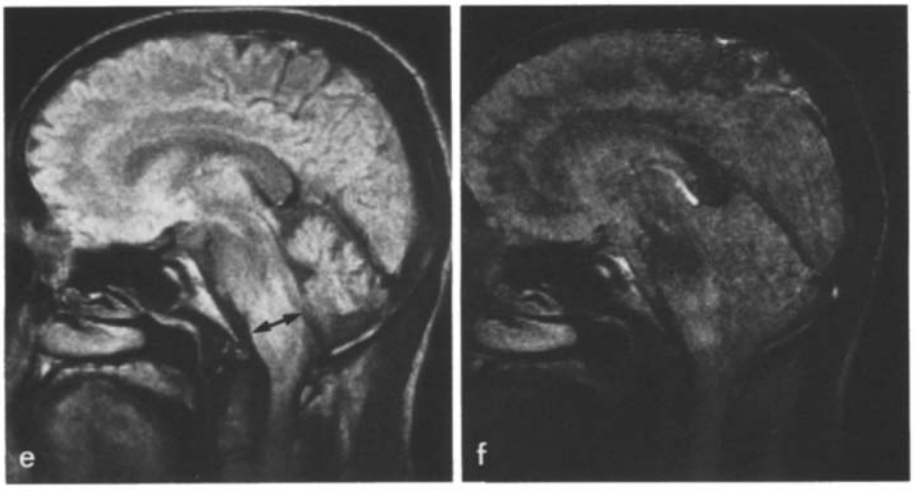

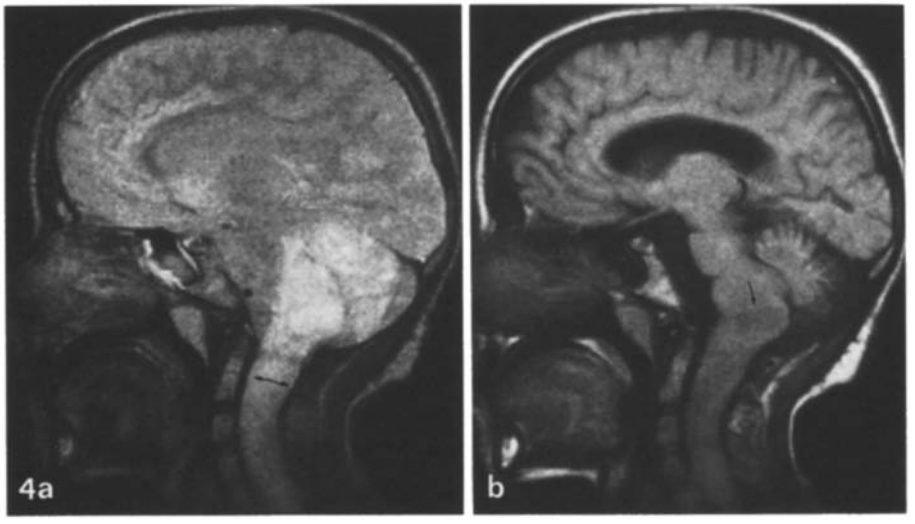

Fig. 4 and b. case 6. Gangliocytoma involving pons, medulla oblongata and spinal cord. **a** SE 1600/70. The tumor displays a long T2. Its extension into the spinal cord which appears enlarged (↔) is evident. **b** SE 400/35. Parts of the tumor are now no longer visible. They have the same signal intensity as the brain. Other parts show a slight lengthening of T1 (→). The deformation of the brainstem as well as the compression of the IV. ventricle and cerebellum are clearly demonstrated

less clearly visible, showing either the same signal intensity compared to the normal parenchyma or slightly decreased signal intensity compared to the normal brain. Nevertheless, the SE 400/35 was very useful in demonstrating the different components of the tumor and also made it possible to exclude hemorrhage and to study the anatomical structure. Anatomical details were particularly well reconizable on IR 1500/400 sequences, but this sequence was seldom used because of the amount of time consumed. Examples are demonstrated in Figures 1, 2, 4, 5.

4. We saw no correlation between signal intensity and type of tumor. The signal was frequently inhomogeneous showing different components of the tumor (Figs. 4, 5). Particularly in the case of angioblastoma (Fig. 2), we could clearly distinguish the cystic from the solid part of the tumor.

5. In all cases, the full extent of the lesion was shown in the axial plane and particularly well in the sagittal plane. In particular, the involvement of the caudal part of the brain stem, which is difficult to appreciate on CT, was clearly recognized on NMR (Fig. 3).

6. In one case (Fig. 4), there was evident involvement of the cervical spinal cord. In one patient (Fig. 2), the canalis centralis appeared enlarged.

7. CT was performed in all cases, and it was always pathological. In two patients (cases 5 and 7), the tumor in CT was only suspected on the basis of compression of the IVth ventricle, enlargement of the brain stem or areas of decreased density (Fig. 3). In 5 cases (patients 3, 4, 6, 8, 9), there was enhancement in the tumor area. In two cases, no contrast was given (patients 1 and 2). In general, the enhancement in CT was smaller than the lesion demonstrated on NMR (Fig. 5), where the full extent of this was clearly better visualised.

Angiography was performed in four patients with enhancement on CT. A rich pathologic vascularisation was recognizable in one astrocytoma

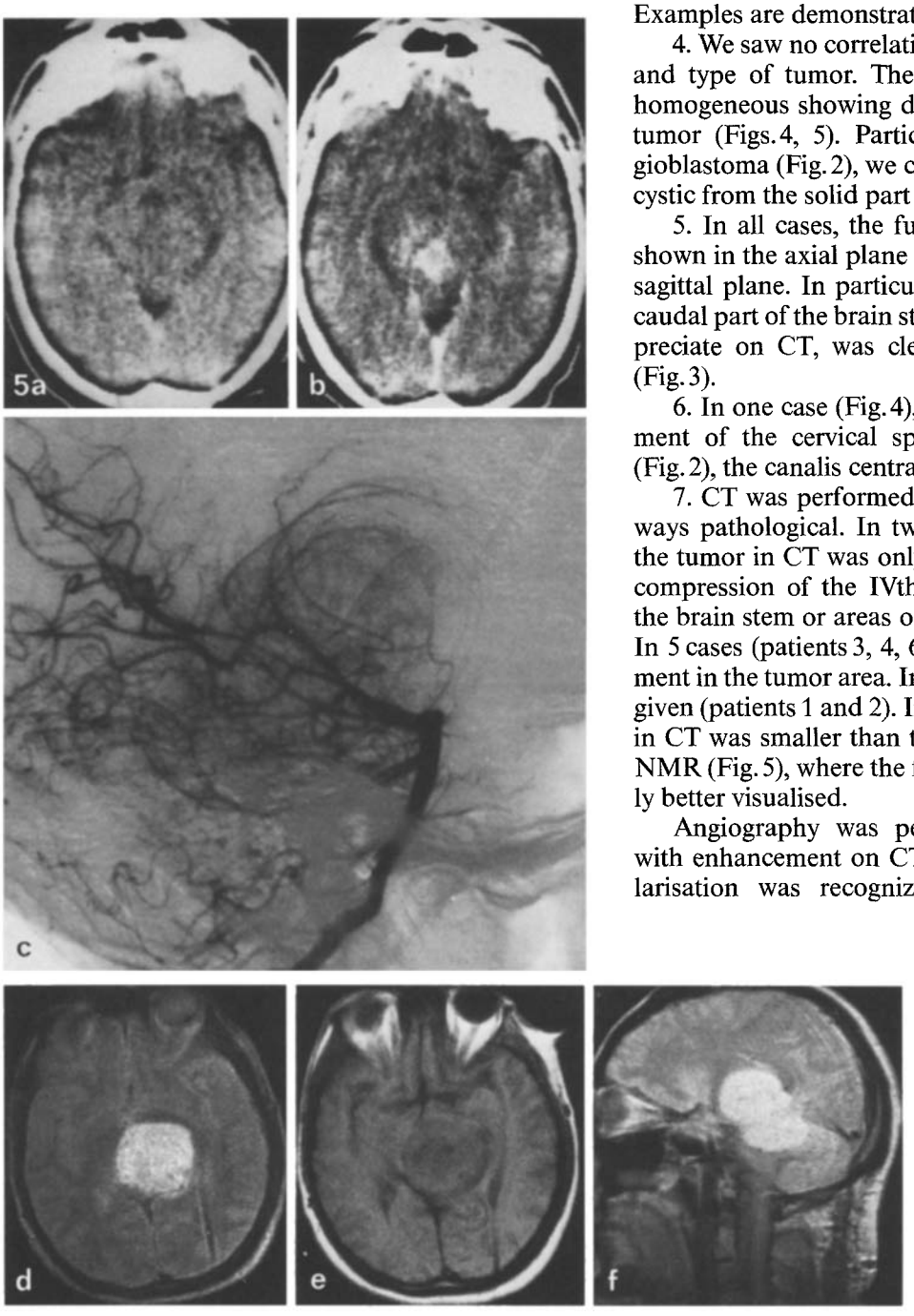

Fig. 5a–f. case 3. Astrocytoma involving thalamus, midbrain and partially the pons. **a, b** On CT, there is an evident enlargement of the midbrain. Parts of the tumor show contrast enhancement (**b**). **c** Pathologic vascularisation on the angiogram. **d, e** NMR. The same axial planes as shown in CT. **d** SE 1600/70. A lesion displaying a long T2 and appearing larger than the enhanced area visible in CT, is recognizable. Since in CT, we do not have the impression that there is edema around the tumor, we can assume that what we recognize on NMR is probably the tumor in its full extension. **e** SE 400/35. Different signal intensities due to areas with different lengthening of T1 are visible. **f** SE 1600/70. Sagittal plane. The full extent of the tumor is well demonstrated

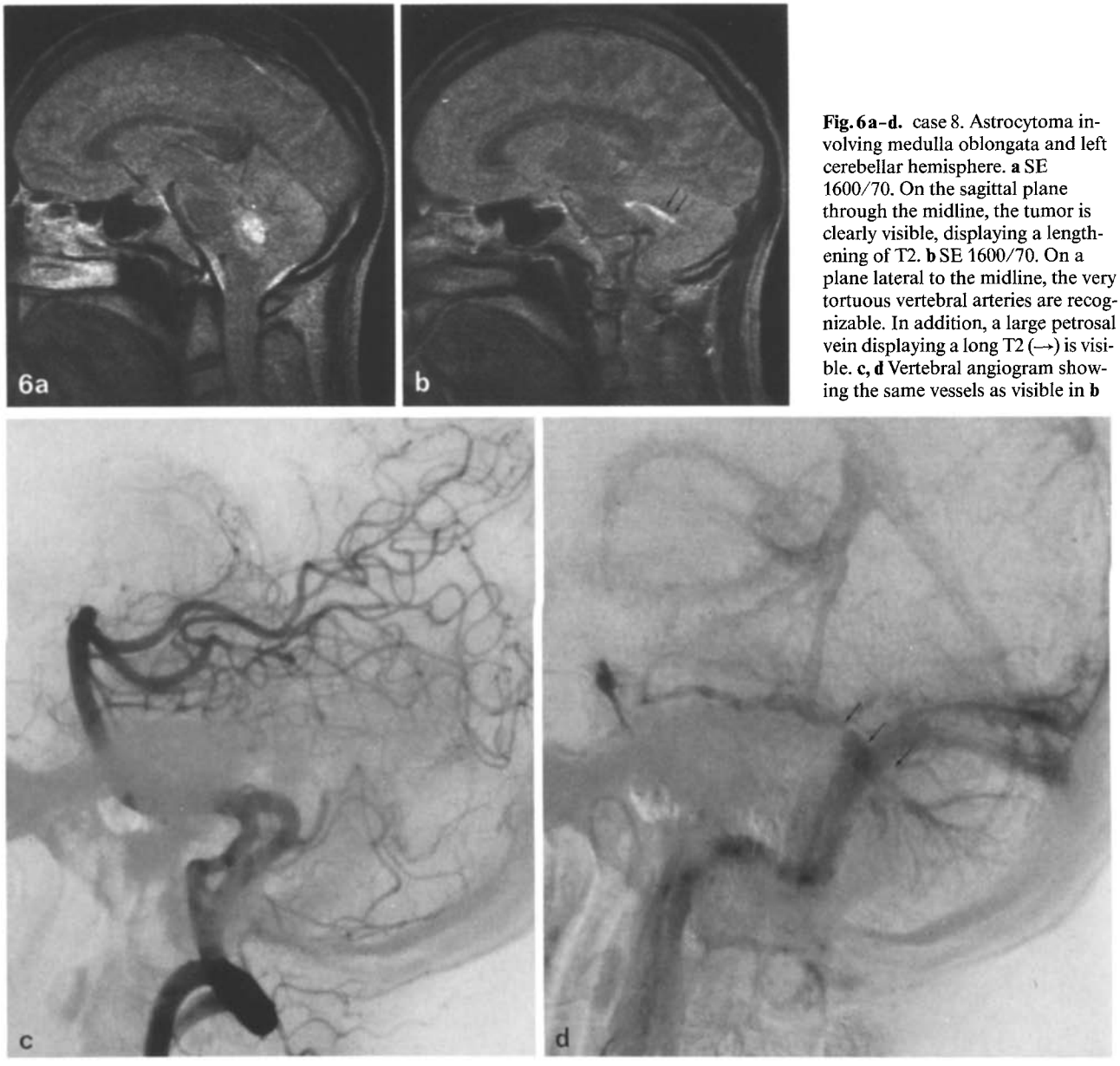

Fig. 6a–d. case 8. Astrocytoma involving medulla oblongata and left cerebellar hemisphere. **a** SE 1600/70. On the sagittal plane through the midline, the tumor is clearly visible, displaying a lengthening of T2. **b** SE 1600/70. On a plane lateral to the midline, the very tortuous vertebral arteries are recognizable. In addition, a large petrosal vein displaying a long T2 (→) is visible. **c, d** Vertebral angiogram showing the same vessels as visible in **b**

(case 3) and in one angioblastoma (case 9). In a third patient, NMR demonstrated elongated and tortuous vertebral arteries. In addition, a linear structure with a long T2 was visible. On the angiogram, this appeared to be a large petrosal vein (Fig. 6).

Discussion and conclusion

In spite of technical improvement of CT, the diagnosis of brain-stem tumors remains relatively difficult with this technique. In the posterior fossa, artefacts are not completely eliminated; frequently the tumor shows no enhancement, and it can be isodense, so that the only evidence for the lesion is a compression of the IVth ventricle and/or enlargement of the brain stem, signs which in many cases are barely discernible. Moreover, even in cases where the diagnosis is certain, the true extent of the tumor and its precise relationship with adjacent structures cannot be fully appreciated in CT.

These difficulties can be overcome with NMR. In our patients, a precise delimitation of the lesion was always possible. It may be problematic in some cases to differentiate between tumor and edema, as already reported by others [4, 6]. Correlation with CT may be useful for this purpose. Contrast medium applied to NMR will perhaps clarify this aspect.

Concerning the type of the lesion a definite diagnosis seemed, in general, not possible in our series, although the demonstration of different components of the tumor and its precise localisation was useful in the interpretation of its possible nature.

In conclusion, our study, like previous reports [3, 5, 6], seems to confirm the high diagnostic value of NMR in investigating brain-stem tumors. This technique is superior to CT and angiography. Nevertheless, these latter examinations remain important diagnostic methods, CT as a screening investigation and angiography for use in selected cases, particularly if enhancement is present in CT.

References

1. Brant-Zawadzki M, Norman D, Newton TH, Kelly WM, Kjos B, Mills CM, Dillon W, Sobel D, Crooks LE (1984) Magnetic resonance of the brain: the optimal screening technique. Radiology 152: 71
2. Bydder GM, Steiner RE, Young IR, Hall AS, Thomas DJ, Marshall J, Pallis CA, Legg NJ (1982) Clinical NMR imaging of the brain: 140 cases. AJR 139: 215
3. Han JS, Bonstelle ChT, Kaufman B, Benson JE, Alfidi RJ, Clampitt RT, Van Dyke C, Huss RG (1984) Magnetic resonance imaging in the evaluation of the brainstem. Radiology 150: 705
4. McGinnis BD, Brady TJ, New PFJ, Buonanno FS, Pykett II, DelaPaz RL, Kistler JP, Taveras JM (1983) Nuclear magnetic resonance (NMR) imaging of tumors in the posterior fossa. J Comput Assoc Tomogr 7: 575
5. Peterman SB, Steiner RE, Bydder GM, Young IR (1984) Evaluation of brain stem tumors with MR imaging. 3rd Annual Meeting of Soc Mag Res Med, New York
6. Randell CP, Collins AG, Young IR, Haywood R, Thomas DJ, McDonnel MJ, Orr JS, Bydder GM, Steiner RE (1983) Nuclear magnetic resonance imaging of posterior fossa tumors. AJNR 4: 1027

Received: 16 November 1984

Prof. Dr. G. B. Bradac
Sektion Neuroradiologie
Radiologische Abteilung
Klinikum Steglitz
Freie Universität Berlin
Hindenburgdamm 30
D-1000 Berlin 45
Federal Republic of Germany